REMOTE SENSING OF PRODUCTIVITY IN NORTHEASTERN FORESTS

A Thesis Presented

by

Aiko S.Weverka

to

The Faculty of the Graduate College

of

The University of Vermont

In Partial Fulfillment of the Requirements
for the Degree of Master of Science
Specializing in Natural Resources

October, 2012

ACKNOWLEDGEMENTS

TABLE OF CONTENTS

LIST OF TABLES

CHAPTER 1: Literature Review

1.1. Forests in the Northeast

In the northeastern United States, forests are an important cultural, economic, and ecological resource. They provide recreational opportunities, non-timber forest products, and aesthetic beauty. Through direct forest-products manufacturing and forest-related tourism, they contribute approximately $19 billion annually to the economies of Maine, New Hampshire, New York and Vermont (North East State Foresters Association 2007). In addition to providing wildlife habitat, forests also perform crucial ecological services, including water filtration (Stein et al. 2009) and carbon sequestration (Goodale et al. 2002, Environmental Protection Agency 2010).

Forests in this region, however, also face an array of different stressors. Soil acidification associated with air pollution has been observed in the decline of certain species and the wider ecosystem (Driscoll et al. 2001). Established exotic insects and pathogens such as gypsy moth and beech bark disease, as well as newly invading pests such as the hemlock-woolly adelgid, emerald ash borer, and Asian long-horned beetle, are projected to have major effects on forested ecosystem processes (Lovett et al. 2006), with anticipated increases in frequency and severity of infestations and outbreaks (Allen 2009, Dukes et al. 2009). Increases in the frequency of severe weather events such as wind and ice storms (Dale et al. 2001) are predicted to lead to the decline of certain tree species, whereas changes in temperature and precipitation patterns may expand or limit the range of others (Iverson and Prasad 1998). Other studies, however, suggest that recent

widely observed forest declines are attributable to natural population senescence, as the majority of trees in the Northeast regenerated at roughly the same time (Wargo and Auclair 2000).

Given the presence of these different stressors, and concerns that forest mortality may be on the rise (Vermont Department of Forests 2010), monitoring is an important step in forest protection. Common forest monitoring methods include field-based studies and aerial surveys, but these are often limited by restricted scalability to the broader landscape and lack of temporal continuity (Zhang et al. 2011). Other potential methods of monitoring forests include dendrochronology studies and remote sensing.

1.2. Dendrochronology

Dendrochronology, the study of annual growth rings produced in trees, can be used to record environmental processes and monitor changes over time (Speer 2010). In temperate climates, trees produce new xylem tissue ovngw xyϑtcownringegs 292..te<004A>10<0048>4

can be used to help monitor and quantify forest health by identifying the timing of specific disturbance events as well as more general tree stress levels given the relationship between prolonged reductions in radial growth and increased mortality risk (Wyckoff and Clark 2002).

Discrete disturbance events can be identified and placed in a larger context through the study of tree-ring patterns. In their research on pandora moth (*Coloradia pandora*) in Oregon, Speer et al. (2001) successfully developed an outbreak "signal," using knowledge of recent moth outbreaks, that was characterized by a precipitous reduction in ring-width that persisted for multiple years. With this outbreak signal, they identified similar occurrences over a 600+ year time span in 14 old-growth stands. The length and geographic scale of these tree-ring chronologies put recent pandora moth outbreaks in greater context and highlighted the potential role of historical processes and climate variation on the moth's population dynamics. Similar research identifying past pine beetle (Kulakowski et al. 2003), forest tent caterpillar (Sutton and Tardis 2007), and ciacada (Speer et al. 2010) outbreaks have been used to recreate the timing and relative severity of outbreaks.

Dendrochronology can also be used to identify specific occurrences of fire and drought. Swetnam and Baisan (1996), and Niklasson and Granström (2000) used burn scars present in tree-ring chronologies to reconstruct past fire history in the Southwestern United States and boreal Sweden respectively. Both of these studies revealed that the lack of fire in the region in the 20th century has been fairly anomalous and coincided strongly

modern precipitation and temperature measurements, and subsequently used this

relationship to reconstruct nearly 800 years of drought occurrence history across North

America. This long-term reconstruction illustrates the ability of tree-rings to track the

spatial and temporal location of both short-term drought events (e.g., <5-10 year) as well

finding is particularly helpful to forest ecologists when studying areas where there is little recorded information about past disturbance history—a common occurrence for most forested regions.

In the Northeast, dendrochronology has been particularly used in the study of decline associated with acid deposition and winter injury. Local observations of red spruce (*Picea rubens*) decline since the 1960s and 1970s (Siccama et al. 1982) were shown to be quite widespread based on reductions in basal area increment measurements observed in 3,000+ trees cored in Vermont, New Hampshire, Maine, and the Adirondacks of New York in the 1960s-mid1980s relative to the previous 50 years (Hornbeck and Smith 1985). Research by Cook et al. (1987) using red spruce tree-ring widths and reconstructed climate records from these chronologies, suggested that these observed trends in growth reduction were not attributable to climate alone, implicating an external factor (i.e., air pollution and acid deposition). However, using these same climate reconstructions they also identified unusually cold winters as an inciting factor in red spruce decline. Similarly, work by Schaberg et al. (2011) examining the effects of a 2003 winter injury event found red spruce foliar dieback was significantly related to reductions in radial growth for multiple years. Notably, this work also identified trees with little evidence of foliar damage after the 2003 event that nevertheless had up to 31% reduction in radial growth. This hints at the complexity of environmental factors that influence growth and illustrates the cumulative effects of an entire growing season (and previous growing seasons) on final tree-ring width.

Halman et al. (2011) also examined the effects of a widespread winter injury event in the Northeast—the 1998 ice storm—on the crown vigor and radial growth of twelve paper birch sites. By measuring calcium depletion in soils at these sites, which has been shown to be linked to acid deposition from air pollution, they found there was a significant association between higher calcium concentrations and stronger recovery of both foliage and basal area increment following damage from that storm. Combining dendrochronology techniques with visual crown assessments and soil chemistry data provided a more nuanced and robust picture of paper birch health. Another study that examined forest response to the 1998 ice storm was Smith and Shortle's (2003) work measuring crown loss and radial growth of 347 hardwoods in New Hampshire and Maine. They found that while severe crown loss (>50%) led to significant immediate reductions in radial growth, most individuals showed signs of full recovery in tree-ring width by 2000. For some species (i.e., white ash (*Fraxinus americana*)), crown replacement occurred so quickly that the amount of crown loss in 1998 appeared to have no significant effect on measurements of radial growth 1998-2000. These studies illustrate how dendrochronology can be used to evaluate resiliency and recovery from disturbance, which is important both in the study of forest health as well as from a commercial timber management perspective.

Tree-rings have annual resolution and can provide decades, if not centuries of information about the status of an individual tree or stand, making dendrochronology very well-suited to monitoring forest condition changes over long periods of time (Biondi 1999). Although dendrochronology can provide a wealth of information about the long-

term health, resilience, recovery and/or decline of various forest ecosystems, collecting and processing cores can be a lengthy and tedious process that requires specialized equipment and training. Due to these processing requirements, dendrochronological studies are often limited in their geographic extent. Given these spatial limitations, dendrochronology can be paired with other tools to analyze forest health and productivity at a broader scale.

1.3. Remote Sensing of Forest Health and Productivity

In contrast to the highly detailed, yet localized information provided by tree-rings, remote sensing is a technique that can be used to monitor forests at the wider landscape scale and in areas where field work is not feasible. Remote sensing can be generally defined as "...*the science of acquiring information about the Earth's surface without being in contact with it. This is done by sensing and recording reflected or emitted energy and processing, analyzing, and applying that information*,"(Canada Centre for Remote Sensing 2007). The energy source most commonly utilized by aerial and space-borne remote sensing devices is the electromagnetic radiation emitted by the sun. This radiation, which has discrete contiguous wavelengths, travels from the sun and then interacts with the earth's atmosphere and surface features where it is scattered, transmitted, absorbed or reflected back to the sensor. Different features will interact with the different wavelengths in a unique manner depending on their physical properties and condition. For example plants reflect very little in the blue and red portion of the electromagnetic spectrum due to the presence of chlorophyll$_a$ and chlorophyll$_b$, which highly absorb wavelengths in in the blue and red range to power photosynthesis. In

contrast, blue light cannot penetrate water as effectively as longer wavelengths and is more highly reflected—hence the reason many bodies of water appear bluish to the human eye. Using knowledge of how various features interact with the electromagnetic spectrum, it is possible to classify and evaluate these features within larger images captured by the sensor. It is also possible to mathematically combine measurements of different wavelengths into ratios or other formulas to capture multiple pieces of information about a feature at once, while offsetting potential error associated with atmospheric attenuation and topography.

While there are a variety of sensors whose imagery can be used in remote sensing studies of forest health, imagery from the Landsat program is particularly well suited for this objective (Cohen and Goward 2004). The Landsat program has collected imagery nearly continuously since 1972 when the first sensor placed on a satellite platform for the purposes of studying and monitoring the earth's surface was launched by NASA. The scene size (183km swath) and temporal resolution (16 days) of images captured by Landsat program permit broad geographic and more detailed temporal coverage. Since 1982, with the launch of Landsat 4 Thematic Mapper (TM), spatial resolution has risen to moderate (30m) and the spectral resolution of imagery has expanded to 7 bands (3 visible, 1 near-infrared, 2 mid-infrared, and 1 thermal). Another major advantage to the use of Landsat data is that as of 2008, imagery is provided free-of-cost and is easily accessible.

Landsat imagery has been used to study and classify forest damage for a variety of tree types and stress events. Rock et al. (1986) found they could identify the relative

degree of damage (high v. low) to red spruce-balsam fir stands in northern Vermont with

high accuracy (r^2 = 0.94-0.95) using a moisture stress index derived from Landsat 5 TM

data. However, it remained ambiguous exactly what biophysical mechanism (e.g., water

stress, cell structure, leaf biomass) was driving the observed differences in the imagery.

Landsat 5 TM imagery has also been used to identify areas experiencing the initial stage

of mortality (reddening of needles) associated with mountain pine beetle attack in British

Columbia (Franklin et al. 2003). For the single year considered (1999), using a

supervised classification with 360 ground truth points, Franklin et al. successfully

distinguished attacked from non-attacked areas with 73% accuracy. Similarly, Nakane

and Kimura (1992) utilized Landsat 5 TM imagery to map Japanese red pine (*Pinus*

densiflora) blight. Using their model, they were able to correctly classify field sites to one

of five damage classes 62% of the time, and to the correct or an adjacent damage class

96% of the time.

In addition to classifying and quantifying damaged areas from a single year, it is

also possible to track changes in forests over time using Landsat imagery from different

months or years. This is particularly useful when attempting to map damage extent, as it

is possible to compare imagery pre-event to post-event imagery. In the Northeast, this

type of analysis has been carried out by many researchers studying discrete disturbance

events. In one of the earlier applications of Landsat TM technology for change forest

detection, Vogelmann and Rock (1989) used imagery from 1984 and 1988 to identify

deciduous forested areas affected by an outbreak of pear thrips *(Taeniothrips*

inconsequens) in southern Vermont and western Massachusetts. Using ground-based

that monitor forest condition over longer time scales than a few years. One example is the work done by Cohen et al. (2002) who used change detection on 11 years of Landsat images over a 23-year period (1972-1995) to identify areas associated with fire and harvesting activity in western Oregon. Given the relatively severe impact of fire and harvesting events on vegetation's spectral response, they were able to distinguish disturbed areas from non-disturbed areas with high (87.8%) accuracy. By combining these Landsat-based maps of forest disturbance with additional data, they tracked rates of disturbance over time as well as by land ownership patterns. Vogelmann et al. (2009) also studied forest condition over a long time period (1988-2006), but in this case were attempting to see more gradual changes in forest health, rather than abrupt disturbance from discrete events (e.g., fire or timber harvest). Using eight Landsat TM images over an 18-year period, they were able to track changes in reflectance over time and found significant declining forest condition trends in their study area in New Mexico. While no quantitative ground-truthing was carried out, inspection of the modeled declining areas suggested that insect dew Mexico. Whil(Vod5>8 m1M23ETBTa mode)4(led ETBd)-5(ou1 0 0 1h 201.65

of the best fit linear trend line of those condition values plotted over time. Analysis of the resulting forest health trend model suggested that at the landscape scale, while there have been fluctuations in forest condition from year to year, overall there is no trend towards improvement or decline. At smaller scales, however, they found that there were localized patches of declining forest, much of which seemed to be associated with higher elevations and balsam fir- paper birch- red spruce communities (Olson 2011). However this model, like the one created by Vogelmann et al. (2009), has not be explicitly ground-truthed, making it difficult to gain a full picture of what ecological processes the Landsat imagery is recording.

Remote sensing studies designed to monitor forest condition over multiple years can be difficult to ground-truth, however, this is an important step given the complexity of processing remotely sensed images and the discrepancies between lab-findings and applications in the field (Hunt and Rock 1989, Pierce et al. 1990, Huete et al. 1994, Cunningham et al. 2009). There are few publically available, spatially explicit, long-term datasets that measure tree canopy condition, which is what the Landsat sensor is "seeing," over time. The

High Resolution Radiometer imagery (AVHRR). They compared tree-rings from a single site in Alaska dominated by birch and spruce to those NPP models 1982-1990, finding moderate positive correlations when comparing raw ring widths (r = 0.366-0.419) and strong correlations after detrending the tree-ring data (r =0.791-0.812). While this comparison was only carried out at one site (as a component of a larger study on productivity), the authors did highlight characteristics of tree-ring data they speculated would be most successfully correlated with NDVI. They suggest analyzed cores should be representative of the growth patterns, species composition, and age class distribution of all trees in the pixel of imagery the samples were collected in.

Using one of these same NPP models derived from NDVI over the same time period (1982-1990), D'Arrigo et al. (2000) came to similar conclusions when comparing maximum latewood density and tree-ring width to NPP at four sites in Alaska and Siberia. Correlation between NPP and a tree-ring width index was moderate to strong for all sites (r   0.59-0.83), however, in this case detrending the tree-ring data actually lead to poorer correlation (r = -0.16- -0.19). Another interesting finding from this study was that the relationship between tree-ring metrics and NPP derived from NDVI was significant and strong in areas where the percent cover of the species cored was relatively rare (10%- 63%). Based on their findings, the authors speculate that strongest relationship between tree-ring increment and NDVI will be observed in areas with a similar limiting growth factor for all species (e.g., temperature or water). This is because poor or strong growth of the species of interest will be mirrored by other (i.e., non-cored)[.)-. . . . . tlslation (r =r offluJET. The

In 2004, the Global Land Cover Facility of the University of Maryland developed a multi-year bi-monthly model of NDVI 1981-2006, based on AVHRR imagery, with worldwide coverage known as the GIMMS (Gobal Inventory Modeling and Mapping Studies) NDVI dataset. With the creation of this dataset, it was possible to easily compare NDVI to tree-ring metrics without significant digital image processing requirements. This facilitated several more studies comparing NDVI to tree-ring data, again in boreal forests, with

found a consistently positive correlation between growing season NDVI

measurements from October. This is in contrast to their findings that deciduous sites

north of 40ºN had positive corre

potential for shrubs to contribute to the NDVI signal, but also suggests that the variability

of NDVI may make interannaul comparisons difficult, depending on imagery timing.

One of the few studies that has used imagery with moderate spatial resolution to

derive NDVI estimates is the work carried out by Babst et al. (2010) on mountain birch in

Sweden. In this complex study on the effects of autumnal moth (*Epirrita autumnata*) on

tree-ring increment, they used three Landsat images (5TM and 7 EMT+) of three

outbreak years and one Indian Remote Sensing Satellite (IRS) image in a year with no

insect damage as a control. Comparing changes in NDVI between outbreak and normal

years and changes in ring widths in outbreak and normal years for seven sites they

developed a third degree polynomial regression model with an r^2 of 0.64. The imagery

used in this study was high enough resolution (23m-30m) to capture disturbances that

happen at smaller or patchier spatial scales, such as the defoliation caused by this moth

outbreak. It is interesting to note they found the change in NDVI was linear to leaf area

lost, but the radial reduction in growth was not. This disconnect between defoliation and

and Goward 2004). Recently Pontius et al. (in prep.) processed 27 years of Landsat imagery that covers eastern New York, Vermont, New Hampshire, and Maine. Using this imagery they were able to track changes in forest health using a newly developed vegetation index that is a combination of multiple hyperspectral indices adapted for multispectral imagery. This model as well as the suite of 49 additional vegetation indices derived from the same imagery 1984-2010, have yet to be ground-truthed to any metric of forest condition on the ground—a crucial step in assessing the limitations of a model.

Taking advantage of the relationship between environmental conditions/stress and radial tree growth, tree-rings have been used in a wide range of forest health studies throughout this region and the world. As tree-rings can provide long-term, nearly annual data they are a good source of information about past forest condition. This thesis research compares tree-ring data from 47 sites in Vermont and New Hampshire to vegetation indices derived from Landsat imagery to evaluate how well the latter corresponds to ground conditions of growth. Although previous authors have examined the relationship between radial growth and a single vegetation index (NDVI) with overall good (though varying) success, the majority of that research has been carried out in boreal forests with remotely sensed imagery that has much coarser spatial resolution than Landsat (Malmström et al. 1997, D'Arrigo et al. 2000, Kaufmann et al. 2004, Kaufmann et al. 2008, Forbes et al. 2009, Lloyd et al. 2010, Berner et al. 2011). Results of this research should provide more information about how well Landsat imagery can be used to monitor forest condition and productivity in temperate, Northeastern forests.

CHAPTER 2: Remote sensing of forest productivity in Northeastern forests

2.1. Introduction

Forests provide a range of goods and services including wood production and carbon sequestration. The ability of trees to perform these functions is dependent on many factors including water and nutrient availability, climatological factors, and both biotic and abiotic disturbances. Monitoring forests is a crucial step in ensuring forests remain biologically

with atmospheric interference and differences in illumination. The normalized difference vegetation index (NDVI), a combination of the red and near infrared portions of the electromagnetic spectrum, is one of the most commonly utilized vegetation indices and has been applied in the study of forest land use change, carbon storage, and biomass estimation (Maselli 2004, Myeong et al. 2006, Meng et al. 2009). There are many other vegetation indices designed for multi-spectral Landsat data that were developed to measure a range of features associated with forest condition including canopy water content

models of global

(Wang et al. 2004, Kaufmann et al. 2008) and

averaged, and then all trees at each site were averaged. In cases where multiple species

had been sampled at a site, we used species basal area (calculated using DBH field

measurements of all trees > 12.5 cm diameter in a 17m radius plot) to calculate a

weighted average BAI.

2.2.3. Remote Sensing

In order to compare field measured BAI at each plot, to spectral reflectance

metrics, imagery from the Landsat 5 Thematic Mapper (TM) sensor was obtained from

the US Geological Service Global Visualization Viewer (http://glovis.usgs.gov/). For

each of the 27 years imagery is available (1984 – 2010) we downloaded one growing-

season (i.e., June 10-August 20) image for two Landsat scenes covering our study area:

Row 29-path 13 (Vermont/ New Hampshire) and row 29-path 14 (eastern New

York/Vermont) (Table 2). A single growing-season image was deemed sufficient to

capture the spectral characteristics of that year's vegetation based on previous finding   É i _

several additional processing steps were required to normalize reflectance across the

imagery time series. We first converted raw digital number (DN) values to top of

atmosphere reflectance to account for differences in illumination intensity and sun angle

among acquisition dates using ENVI 4.8 (Exelis 2011, Colorado Springs, CO).

Calculation of many of the vegetation indices explored in this study required an

additional conversion to at-surface reflectance. We chose a histogram-based dark object

subtract for each band. This dark object subtract approach has been shown to be as

effective at reducing the differences in surface reflectance estimation between multi-date

images as more complex radiative transfer models for multi-spectral imagery (Song et al.

2001). To ensure accurate co-registration of pixels across years, we georegistered each

image to a common mid-study cloud-free image using a 3rd order polynomial with a

nearest-neighbor resampling technique (root-mean square error < 0.2 pixels or 6m

average accuracy). Considering the 17m radius field plots and 30 m spatial resolution of

the Landsat sensor this level of accuracy is necessary to ensure correct spectra extraction

for each field plot.

Surface reflectance was extracted for bands 1-5, and 7 using the Spatial Analyst

tools in Arc 10 (ESRI 2011, Redlands, CA) from the closest pixel to the GPS coordinates

of plot center. Cloud cover, haze, and cloud shadow can "pollute" reflectance values as

they mask and alter spectral data. To ensure that only cloud free data was included in our

analysis we visually inspected each site across all images. Extracted values were

manually converted to "NoData" for that year if the site was covered by cloud, cloud

shadow or visible haze in any given image. Given that the two Landsat scenes included in

this study overlap for ~65 km across New Hampshire and Vermont (Figure 2), there were

many study sites with two sets of spectral data available in each year. Where available,

these spectral values were averaged to come up with one set of spectral data per year.

While Landsat band locations were developed with vegetation applications in

mind, there is a wealth of vegetation indices that can improve upon the ability of the

sensor to detect specific canopy biophysical parameters (Table 3). This includes many

broad-band indices, designed specifically using multi-spectral sensors like Landsat, but

also extends to a suite of narrow-band indices designed specifically for hyperspectral

applications, that to our knowledge have not been tested using broad-band sensors.

In order to conduct a comprehensive assessment of Landsat's ability to quantify

forest growth and productivity, we created a spectral database to calculate a suite of

vegetation indices with documented relationships to canopy characteristics. For narrow-

band indices, we calculated a Landsat equivalent where each distinct narrow-band

wavelength required for calculation fell within a distinct Landsat band. For example, the

chlorophyll sensitive index proposed by Datt (1998) calls for a ratio between reflectance

at 672 nm and R550 nm. We calculated a broad band equivalent as Landsat 5 TM

Band3:Band2. While the expectation is that much of the specific information pertinent to

chlorophyll$_b$ content captured in the narrow-band equation will be lost in the broad-band

equivalent due to the narrow chlorophyll$_b$ absorption feature, there may still be enough

information relative to vegetation condition to make it useful in a more complex model.

The resulting database calculated 55 pre-existing vegetation indices/raw bands (Table 3)

including common multi-spectral indices such as the normalized difference vegetation

index (NDVI), and more complex narrow-band indices like the structure insensitive pigment index (SIPI).

2.2.4. Statistical Analysis

As a preliminary data exploration step, annual BAI measurements were compared to annual vegetation indices across all sites and all years 1984-2010 (n =701) using Spearman's rho correlation. While statistically complicated by temporal autocorrelation, and artificially inflated sample size, this analysis was not intended to identify significant relationships, but instead to identify which of the 55 vegetation indices were likely to have a significant relationship with BAI in subsequent analyses. This was of considerable interest based on our goal to develop a global, or "landscape scale," model to quantify forest growth. Such a model would have to maintain relationships across sites of varying species composition and years of varying growth conditions. To explore the strength of fit when analysis was limited to a single species, this test was rerun on 5 species "types"("Red Spruce," "Birch," "Pine," Mixed Hardwoods," and "Mixed Balsam Fir/Red Spruce/ Birch") that were created by combining data from sites with similar species composition.

To measure the relationship between BAI and vegetation indices while accounting for inherent differences in tree-ring series (as a result of different species composition, landscape characteristics, external disturbance etc.) and autocorrelation across years (Berner et al. 2011), we conducted a Spearman's rho correlation across all available imagery years on a site by site basis. Correlation analysis assumes independence among observations—a condition likely to be unmet by tree-ring data

given the effect one year's growth may have on subsequent years. To address the statistical violation of carrying out correlations on datasets with potential temporal autocorrelation across years, the effective sample size was reduced by penalizing the sample size in proportion to the degree of first order autocorrelation between one year's BAI and the following year's BAI (Dawdy and Matalas 1964 adapted by Berner et al. 2011; Appendix A) in R (version 2.15.1). In cases where there was no significant ($p <$ 0.05) autocorrelation, the full sample size was preserved. This site-specific analysis also highlights which types of stands have the strongest or weakest relationships between BAI and vegetation indices, or if different indices are required to quantify growth in different forest types. Due to cloud cover present in the imagery, not all years were available at all sites, further limiting the sample size.

Because woody growth is potentially related to many different canopy metrics (leaf area index, chlorophyll content, leaf moisture content, etc.) it is possible that no single spectral index can be used to quantify forest growth alone. To test this theory, we developed a multi-vegetation index model to predict forest growth across the region (i.e., with data from all sites and all years) using stepwise linear regression. With BAI as the dependent variable, the mixed platform tests all possible linear regressions combinations, retaining vegetation indices that strengthen the model fit. To avoid over-fitting, model development was limited to a maximum of 5 terms (Williams and Norris 2001), < 0.05 for all terms and a variance inflation factor < 10 (Kleinbaum et al. 1998). Jackknifed residuals calculated from the PRESS statistic were also used to assess the stability of the final predictive equation (Kozak and Kozak 2003). Based on preliminary results, an

chlorophyll (NPCI, SIPI, SRPI, MSR705, MND705) (Peñuelas et al. 1993, Peñuelas et al. 1995, Sims and Gamon 2002). Chlorophyll levels are related to a plant's ability to produce carbohydrates and by extension the xylem tissue that forms tree-rings. Chlorophyll fluorescence can be used as an early indicator of leaf stress as it is one of the first indicators of reductions in photosyntheon(5pn befic08.ieuse

tree-ring width index of willows at 27 sites in northern Russia. There are many experimental and ecological explanations for the observed relatively low correlation coefficients, many of which are discussed in section 2.3.4. While these overall associations are relatively weaker, our results show that other vegetation indices outperformed the commonly used NDVI, suggesting that future studies using remote sensing techniques to quantify forest growth should consider expanding the range of indices utilized.

At this "global" scale, plotting out BAI against each significantly correlated vegetation index and color coding data points by species membership (forved rce4ETB56uFi6uFi6u1ETE

growth.

(average r = 0.609 ± 0.078). Among these sites with a significant relationship between

BAI and MIR, there were not apparent similarities with regard to species composition (2

paper birch, 1 mixed hardwoods, 2 red spruce), sample siz

one would expect) with BAI measurements at 7 sites (mean   = 0.481 ± .074, mean p =

0.063 ± 0.023). However, there were two sites that had a significant negative relationship

(which one would not expect) between BAI and NDII7 as well (mean   = -0.479 ± .014,

mean p = .0893 ± 0.013). NDII7 is a combination of the near infrared (band 4) and mid

infrared (band 7) bands (Table 3) (Hunt and Rock 1989) and was developed to evaluate

water content by utilizing the high water absorbance of band 7 (e.g., lower reflectance

signals higher water content) and the cell structure information provided by band 4 (e.g.,

higher reflectance signals healthy intercellular air spaces).

It is interesting that the two vegetation indices (MIR, NDII7) that had a

significant relationship to BAI measurements at the most sites are both associated with

water levels in vegetation. This could be due to a range of different reasons including the

direct association of water stress with reduced radial tree growth (Stahle et al. 2007, Klos

et al. 2009) as well as water stress potentially serving as an indicator of the presence of

other stressors such as insect and pathogen damage (Townsend et al. 2012). Being farther

along the electromagnetic spectrum, the bands that compose these indices (band 4, 5, and

7)

using near-infrared and mid-infrared bands (e.g., NDII7) to monitor actual water levels for a variety of species only worked for very severe cases of water stress. The only field-based study we were able to identify used a simulated Landsat TM sensor mounted on a plane (Pierce et al. 1990) and found the strength of the relationship between the normalized difference infrared index using band 5 in place of band 7 (e.g., NDII5) and field measurements of water pressure varied based on the time of day. The sensor was able to see significant differences between healthy and severely girdled trees in the morning, but in afternoon imagery, no significant difference was visible between stands due to transpiration. Landsat imagery is collected at around the same time of day—approximately solar noon—a point in the day when the differences between normal and water-stressed trees was not still distinguishable in the Pierce et al. (1990) study.

Within-site analysis of the relationship between BAI and vegetation indices should hold constant factors such as species composition, topography, and soil properties that likely contribute variation in that relationship at a broader landscape scale. The fact that relatively few (21% using = 0.05; 36% using = 0.10) of these sites had a significant relationship between BAI and any of the 55 vegetation indices, and that no one index was significantly correlated with BAI at more than 7 sites suggests that there iT1 0 0 1 338.59

mm^2 compared to a mean BAI of 1013.57 mm^2) suggests that it may not be a very useful

model from a predictive standpoint.

measure canopy moisture content, leaf stress, vegetation biomass, and an integrated measure of "forest decline," respectively.

Potential reasons for relatively better modeling success for paper birch include a larger sample size: 12 sites fell into this species type and on average these sites had 19 (± 2.79) years of imagery data available, due in part to all sites falling in both Landsat row 29 / path 14 and row 29/ path 13. The dendrochronological sampling used to collect the tree-ring data was also specifically designed to capture a range of canopy conditions and elevation types, and included many declining trees that were in poor enough condition to have locally absent rings (Halman et al. 2011). By including a broader range of potential growth conditions, relationships between vegetation indices and BAI are more robust. Another potential explanation for the stronger predictive ability of this model compared to the model including all species, is that paper birch do not retain their photosynthetic material from one year to the next, thus reducing complications from a lagged radial growth response related to damaged needles retained from previous years. Lastly, these sites were also relatively close to one another (<50km apart), which means that they may be more likely to share characteristics not accounted for in the modeling process, that nevertheless likely affect BAI including precipitation patterns, storm and winter injury damage, and some soil properties.

The other species type with a large sample size available on which to base a predictive BAI model was red spruce (with 22 sites). Unlike the model developed for paper birch, however, this model (**Figure 7**b) performed more poorly than the global model (p = <0.0001, r^2 = 0.116, adjusted r^2 = 0.107, RMSE = 548.79 with mean BAI =

41

1048.65). The stepwise model fitting process retained the following vegetation indices for the final predictive equation for red spruce: the first derivative of two mid-infrared bands (Landsat band 7 and band 5) (FD75)(

sites also had significant

together spectrally in the imagery. With a longer and wetter growing season, forests in the Northeast also tend to experience catastrophic disturbance with less frequency than other forested ecosystems (Seymour et al. 2002). Less dramatic loss of canopy from disturbance events and relatively quick regeneration of the understory post-disturbance

pick up that loss of biomass. The remaining trees at that site cored in 2010, however, would not have had any sign of reduced growth post- harvesting activity in their tree-ring records, and in fact may have experienced release. This difference between Landsat measurement of forest condition and the record contained in the tree-rings of individuals cored could lead to muddying of their relationship. In this particular example, this site was removed from this analysis to reduce that potential source of error. However, the history of many sites included in analysis remains unknown.

While there are many potential sources of error specific to this study, there is also some evidence that the relationship between canopy condition (which is what the Landsat imagery directly captures) and radial growth is somewhat complicated and non-linear. In a lengthy literature review on forest decline and basal area increment in Europe, Innes (1993) concluded that trees had to lose between 30% and 50% of their foliage before growth reductions were apparent in the tree-rings. There are similar examples of this in the Northeast where Schaberg et al. (2011) found examples of red spruce trees with 100% canopy loss that resulted in only a 60% reduction in radial growth for that year. Work by Smith and Shortle (2003) on hardwoods after the 1998 ice storm also revealed that for certain species (i.e., white ash), the degree of damage experienced

that in some cases tree-ring production stopped up to 30 years before a tree was

as well as variability in the proportion of primary productivity (viewable by the Landsat sensor) that is ultimately allocated to radial trunk growth (tree-rings).

2.4. Conclusions

Statistically significant, although weak, relationships between BAI and some vegetation indices were observed. The most consistently significant indices across the three analyses (defined as either the strongest, or showing up in multiple analyses) include: NDII7, MIR, SARVI, OSAVI, Flo, SRPI, and VogB . These are designed to measure water stress, "greenness" (a combination of biomass, leaf area index, vegetation cover) adjusted for atmospheric and soil interference, and chlorophyll and carotenoid content. While NDVI is a very widely used vegetation index, in our analyses, it appears to have underperformed many other multispectral and hyperspectral indices. The strength of associations and model fit were also improved by focusing on single species types instead of attempting to carry out analyses on all sites, regardless of species composition.

These findings suggest that while remotely sensed products have been shown to be usable in identifying disturbance events (Rock et al. 1986, Vogelmann and Rock 1989, Cohen et al. 2002, Olthof et al. 2004, Townsend et al. 2012), factors such as the timing and availability of imagery, mixed pixel issues common to heterogeneous forests such as those in the Northeast, mortality and regeneration captured in pixels and not in cores, among other factors, may make it difficult to use this imagery to accurately model radial growth. If efforts were undertaken to model forest productivity (in terms of BAI) from

indices beyond NDVI alone and developing species-specific equations as opposed to applying a single equation across an entire image. Any results should also be interpreted with care, understanding that accuracy may only be within 20-25% (proportion of RMSE/mean) of true BAI at best. While limited in absolute accuracy, in this study using a suite of vegetation indices derived from Landsat imagery to predict BAI was an improvement over NDVI alone and could potentially be used as a general relative measure of landscape scale productivity from year to year.

BNT182	VT	A. Kosiba	PIRU	10	12	12	Yes
BNT185	VT	A. Kosiba	PIRU				

RVI   B4/B3   "Greenness"

Table 5

Species Type	Vegetation Index	Spearman rho	p-

Figures:
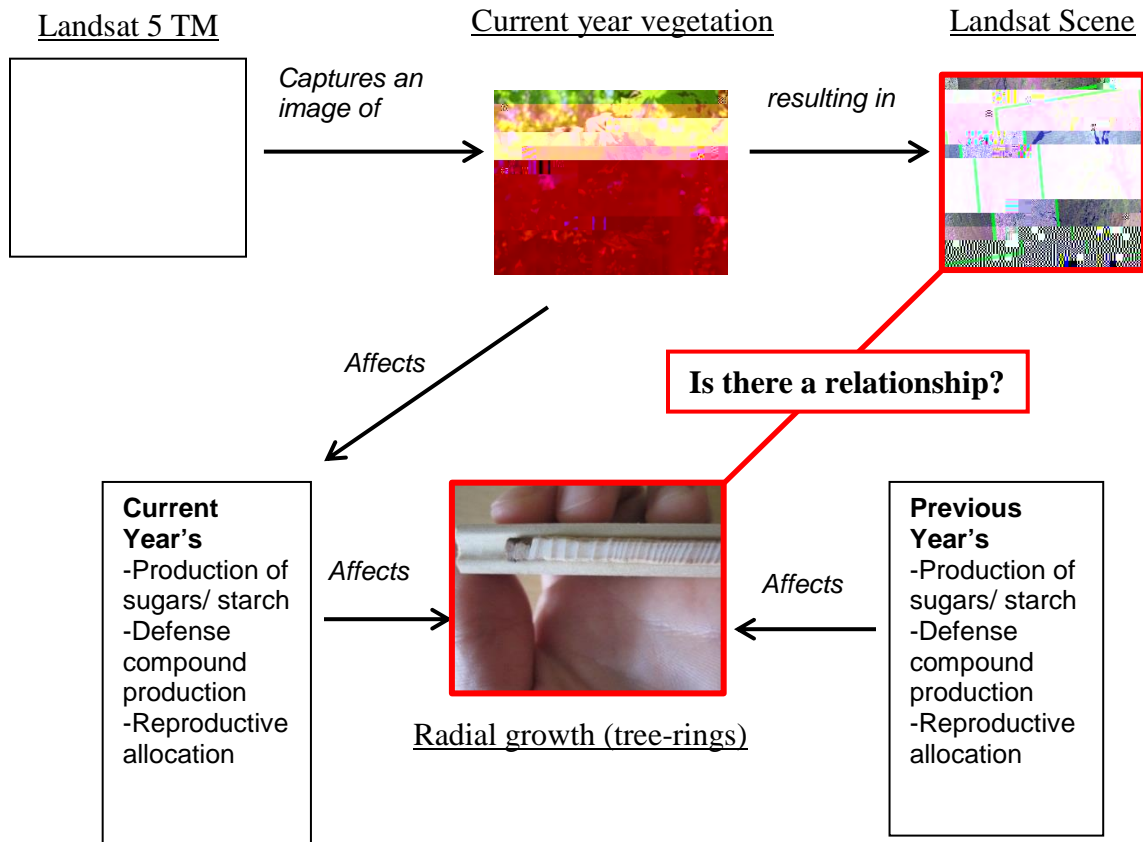
Figure 1: A conceptual model of the hypothesized relationship between Landsat imagery and radial-growth (tree-rings)
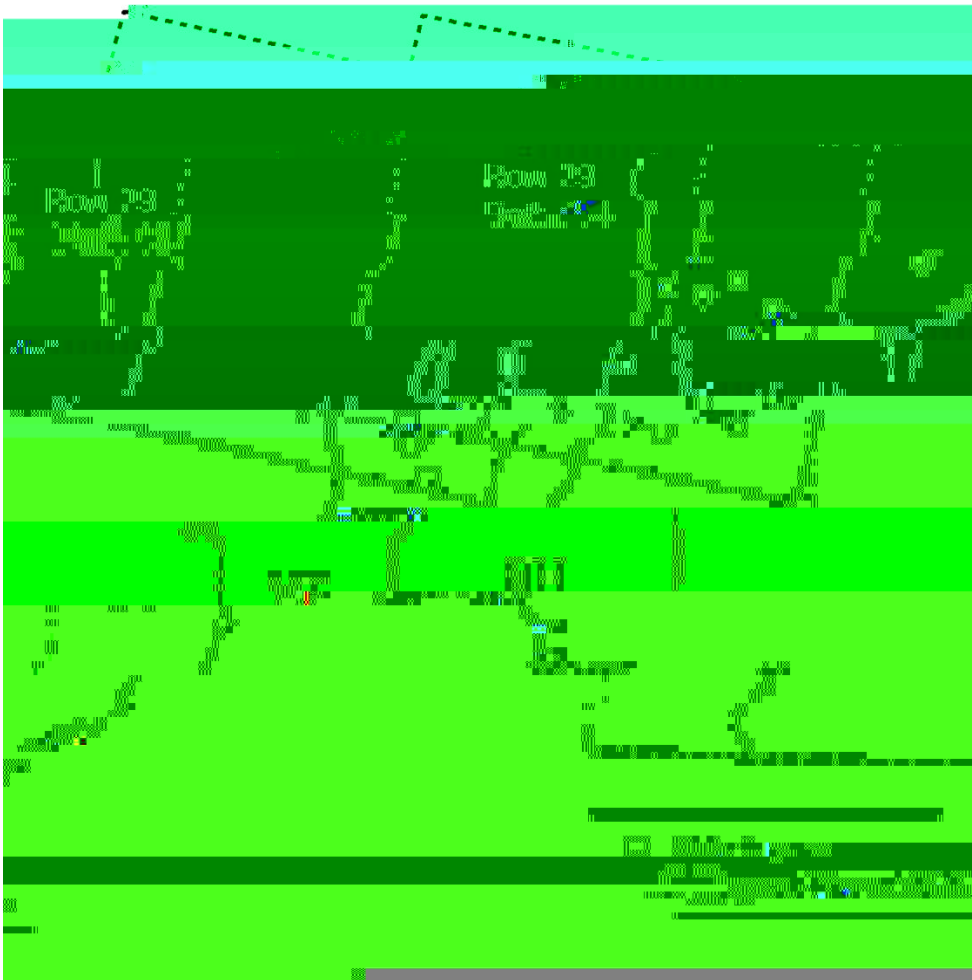
Figure 2: Map of the study region with Landsat 5 TM scene boundaries and site locations
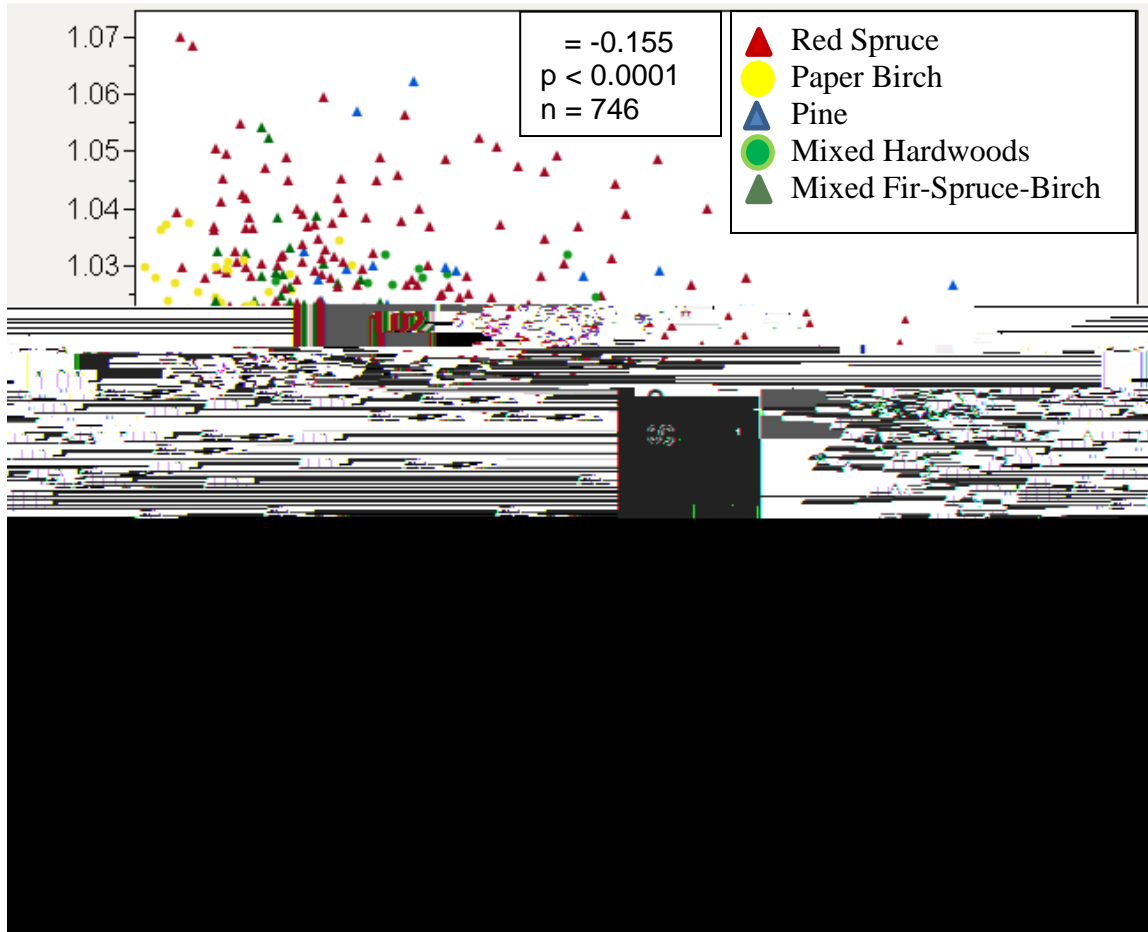
Figure 3: An example of the "global" (all years and all sites) relationship between BAI and vegetation index measurements, in this case the structure insensitive pigment index (SIPI)(Peñuelas et al. 1995). Data points are color coded by species. Note the obvious clustering of similar species types.

Figure 4: BAI vs. NDVI and MIR for two sites: CAM070 (with a significant relationship to MIR) and BAR003 (without a significant relationship to MIR). Gaps in the vegetation index values are years where imagery was not available.
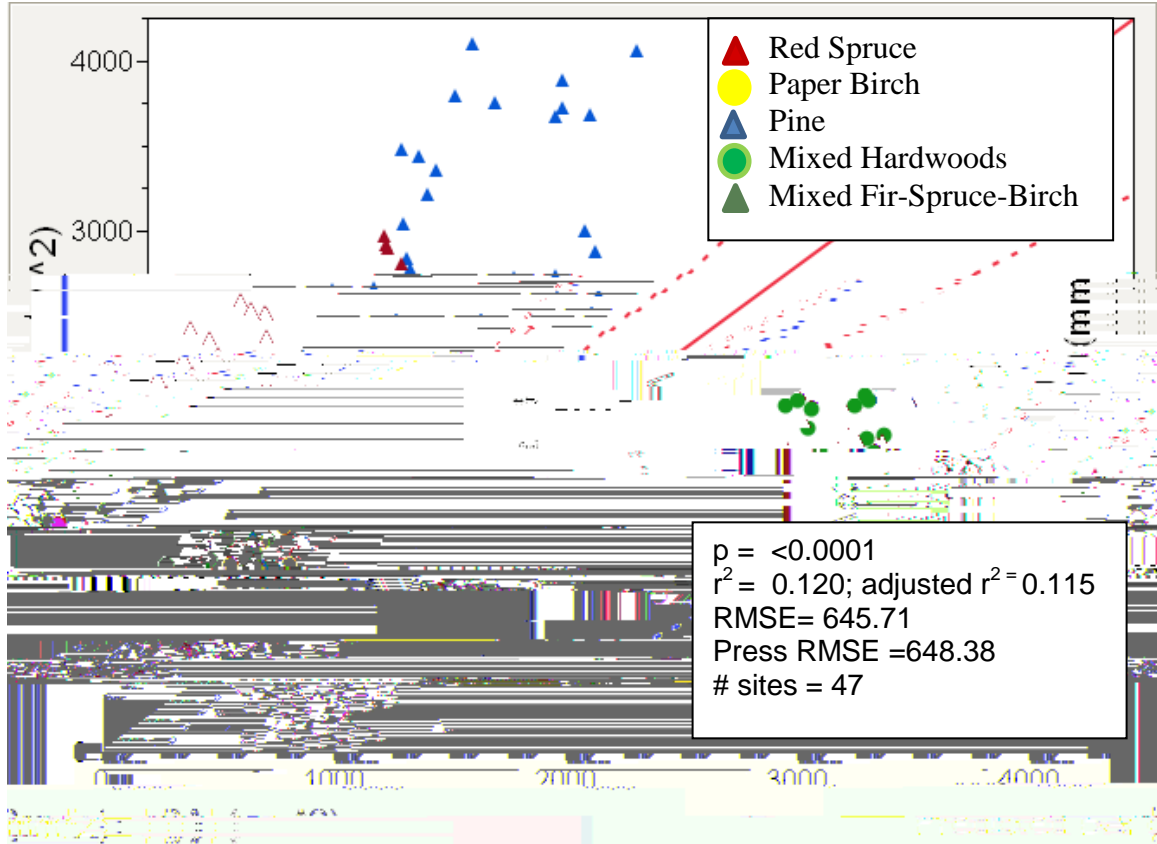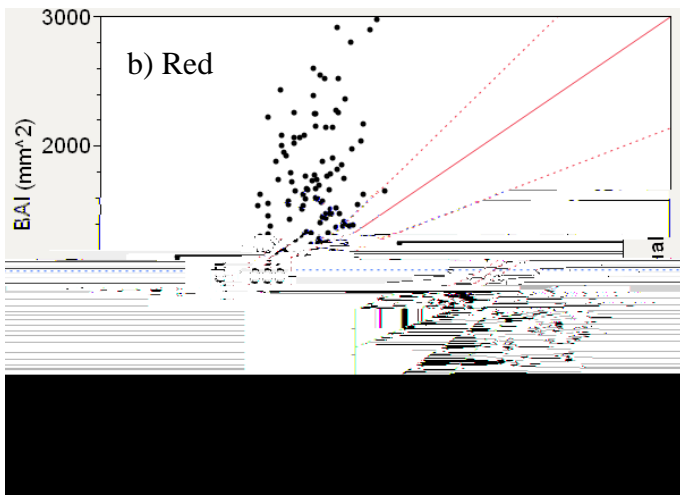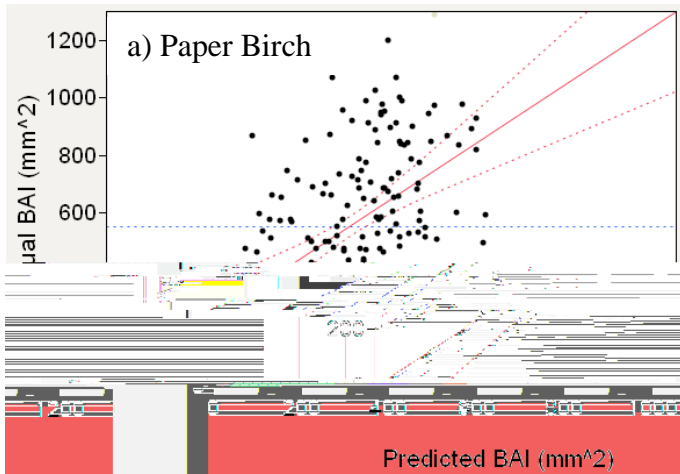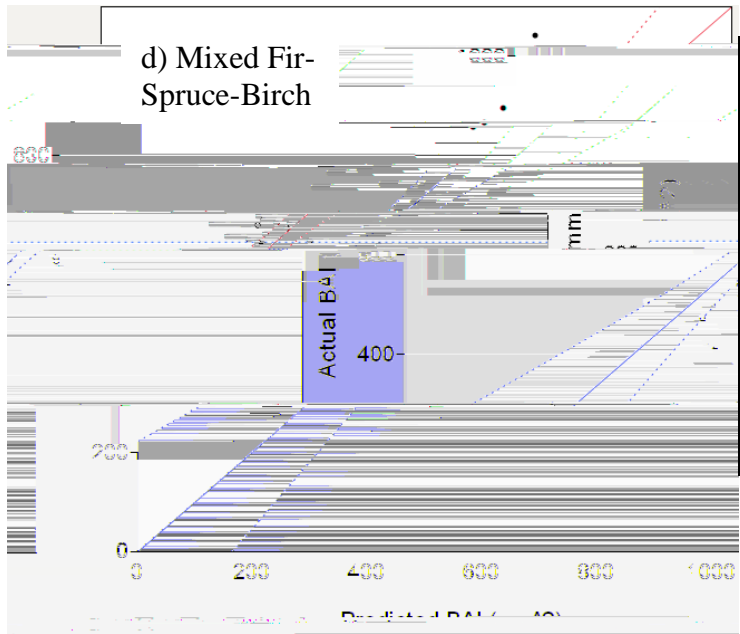
Figure 5: The four-term model that predicts BAI (mm^2) with r^2 = 0.120, RMSE = 645.71 using the following equation developed with data points from all species types and all years: 12148.476 - 61358.22* (**B3**) + 1714.863*(**BNa**) -11198.23*(**MSR705**) - 541.938*(**SRPI**).
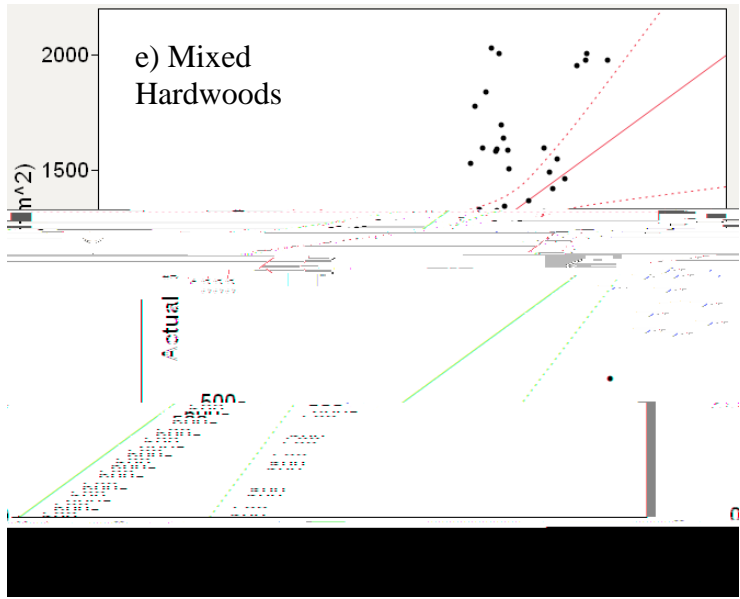
Figure 6: Average residual values from the global model predicting BAI from Band 3, SRPI, MSR705 and

d) Mixed Fir-Spruce-Birch
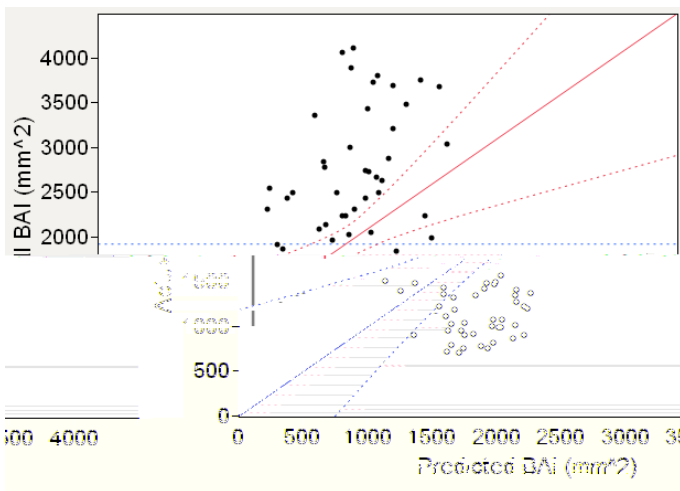
p = <0.0001
$r^2 = 0.311$; adjusted $r^2 = 0.301$
RMSE=131.571
Press RMSE = 133.64655
sites = 4

Equation:
BAI (mm^2) =
 $-213.725 + (SAVI*1818.632)$

e) Mixed Hardwoods

p = 0.0194
$r^2 = 0.094$; adjusted $r^2 = 0.077$
RMSE= 332.64
Press RMSE = 339.81
sites = 5

Equation:
BAI (mm^2) =
 $1016.202 - (SARVI*104.291)$

Figure 7: Actual vs. predictive BAI models developed using stepwise model fitting for the following species types: a) Paper Birch, b) Red Spruce c) Pine d) Mixed Fir-Spruce-Birch e) Mixed Hardwoods.

Appendix A:

R c

Literature Cited:

Allen, C. D. 2009. Climate-induced forest dieback: An escalating global phenomenon? Unsylva **60**:43-39.

Babst, F., J. Esper, and E. Parlow. 2010. Landsat TM/ETM+ and tree-ring based assessment of spatiotemporal patterns of the autumnal moth

Dale, V. H., L. A. Joyce, S. McNutly, R. P. Neilson, M. P. Ayres, M. D. Flanagan, P. J. Hanson, L. C. Irland, A. E. Lugo, C. J. Peterson, D. Simberloff, F. Swanson., B. J.

Olthof, I., D. J. King, and R. A. Lautenschlager, 2004. Mapping deciduous forest ice Environment